Seismic evidence for a lower-mantle origin of the Iceland plume

Yang Shen*, Sean C. Solomon†, Ingi Th. Bjarnason‡ & Cecily J. Wolfe*

** Department of Geology and Geophysics, Woods Hole Oceanographic Institution, Woods Hole, Massachusetts 02543, USA*
† Department of Terrestrial Magnetism, Carnegie Institution of Washington, 5241 Broad Branch Road, NW, Washington DC 20015, USA
‡ Science Institute, University of Iceland, Reykjavik, Iceland

Iceland, one of the most thoroughly investigated hotspots[1–3], is generally accepted to be the manifestation of an upwelling mantle plume[4]. Yet whether the plume originates from the lower mantle or from a convective instability at a thermal boundary layer between the upper and lower mantle near 660 km depth[5,6] remains unconstrained. Tomographic inversions of body-wave delay times show that low seismic velocities extend to at least 400 km depth beneath central Iceland[7,8], but cannot resolve structure at greater depth. Here we report lateral variations in the depths of compressional-to-shear wave conversions at the two seismic discontinuities marking the top and bottom of the mantle transition zone beneath Iceland. We find that the transition zone is 20 km thinner than in the average Earth[9] beneath central and southern Iceland, but is of normal thickness beneath surrounding areas, a result indicative of a hot and narrow plume originating from the lower mantle.

Observational constraints on the deep structure of plumes are sparse, with only one report of the detection of a narrow plume conduit at a depth of ~700 km (ref. 10). A new approach to address the question of the depth of origin of mantle plumes is to map the mantle seismic discontinuities near 410 and 660 km depth, features that have been identified with the transitions from the α-phase to the β-phase of $(Mg,Fe)_2SiO_4$ and from γ-$(Mg,Fe)_2SiO_4$ to perovskite plus magnesiowustite[11], respectively. The depths to the 410- and 660-km discontinuities respectively increase and decrease with increasing temperature, and thus provide information on lateral temperature variations and associated mantle circulation patterns. As sketched in Fig. 1, lateral variations in the discontinuity depths can be diagnostic of the depth of origin of mantle plumes.

The data used here are receiver functions[12] derived from body-wave records of teleseismic earthquakes from the broadband ICE-MELT seismic network[13] and the permanent Global Seismographic Network (GSN) station BORG on Iceland (Fig. 2). The calculation of receiver functions follows procedures previously described[14].

To image lateral variations in seismic discontinuities, we use geographical binning of receiver functions[15]. At a given binning depth beneath Iceland and the surrounding area, we divide the horizontal plane into overlapping square patches (200 × 200 km, Fig. 2), comparable in dimension to the Fresnel zone of a P660s phase (Pds denotes a *P*-to-*S* conversion at depth *d*) of frequency 0.1–0.3 Hz at the conversion depth. Each patch overlaps two-thirds of its area with adjacent patches. For every 10-km increment in binning depth from the surface to 1,200 km, receiver functions having Pds paths that pierce the same patch are gathered (Fig. 2), corrected for moveout to a reference ray parameter of 0.0573 s km^{-1} (ref. 14), and stacked using an *n*th-root method[16] ($n = 2$) in the time window corresponding to the given binning depth interval.

The stacked receiver functions clearly reveal arrivals corresponding to the 410- and 660-km discontinuities (Fig. 3). There is no evidence for a coherent *P*-to-*S* conversion from near 520 km depth[17]. North of Iceland, variations in P410s and P660s times are positively correlated and comparable in magnitude (Fig. 3b). Such a positive correlation reflects velocity heterogeneities shallower than the 410-km discontinuity because of the nearly identical paths of P660s and P410s over that depth interval. P660s-P410s differential times, which provide information on the thickness of the transition zone, are not sensitive to heterogeneities shallower than the 410-km discontinuity and are similar to that predicted by the iasp91 global model[9] (Fig. 3b). The positive correlation between P410s and P660s times breaks down beneath central and southern Iceland (Figs 3c

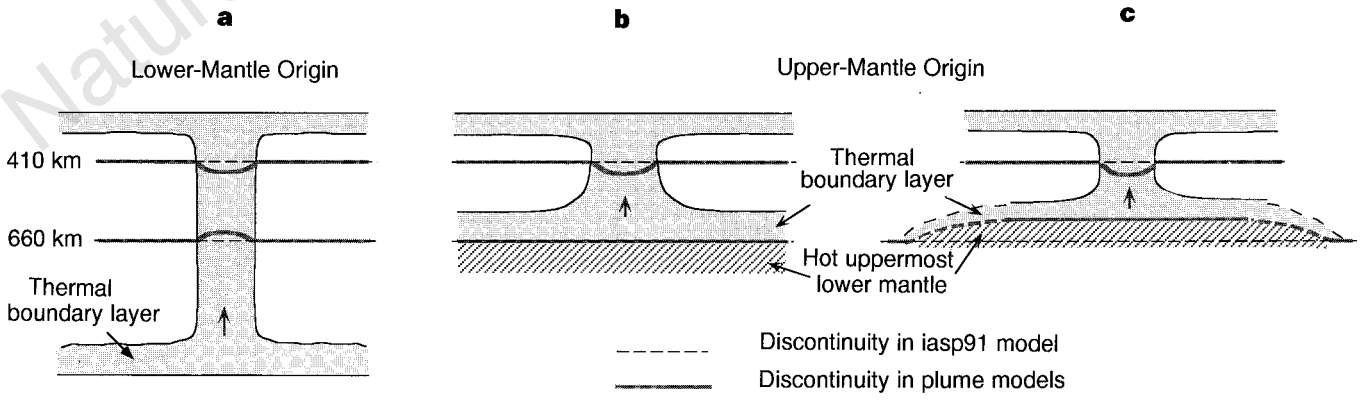

Figure 1 Variations in the depths of the 410- and 660-km phase boundaries can distinguish three generalized, end-member models for mantle plumes, here depicted schematically. Horizontal dashed lines denote 410 and 660 km depth. The seismic discontinuities associated with the phase change are shown as thick lines. The shaded regions represent hotter-than-normal mantle material associated with plumes; the stippled regions represent hot lower-mantle material. **a**, Under the model in which a plume originates from the lower mantle[4], the depths to the 410- and 660-km discontinuities are deeper and shallower than normal, respectively, but only in the immediate vicinity of the plume conduit. **b**, In one type of strongly layered mantle convection model, plumes arise from instabilities in a global thermal boundary layer at the base of the upper mantle marked by the 660-km phase boundary, and lateral variations in temperatures at the base of the boundary layer are generally less than the excess temperature of the plumes[5,19]. The depth to the 660-km discontinuity is thus nearly constant and, by definition, that of the average Earth[9]. The 410-km discontinuity is deeper than normal in the vicinity of the plume conduit. **c**, In another type of layered-mantle convection model, plumes arise from regions of the boundary layer at the base of the upper mantle that are heated by the underlying lower mantle[20]. The horizontal extent of the portion of the boundary layer supplying the plume is much greater than the diameter of the plume conduit, reducing the depth of the 660-km discontinuity, and thus the thickness of the mantle transition zone, over a broad region.

Nature © Macmillan Publishers Ltd 1998

Nature © Macmillan Publishers Ltd 1998

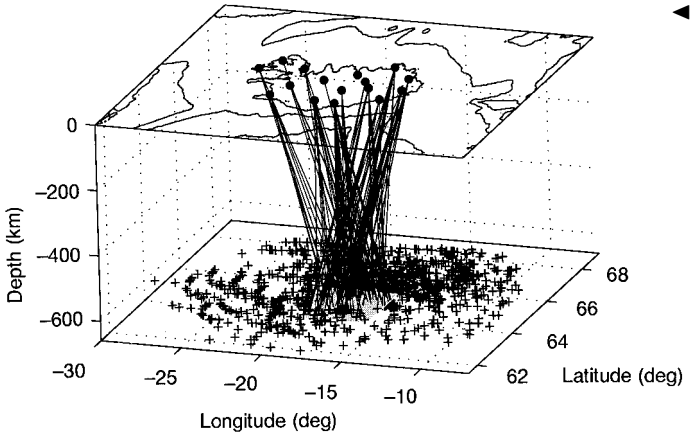

Figure 2 The geometry of our experiment. Shown are the locations of the piercing points of P660s ray paths at the 660-km discontinuity (crosses) and the P660s ray paths (lines) from the central patch (grey square) to the ICEMELT seismic stations and the GSN station BORG (dots). The Icelandic coast and the Reykjanes and Kolbeinsey ridges are represented by regional bathymetry at 1-km contours. A total of 1,560 pairs of radial and transverse receiver functions sample the discontinuity.

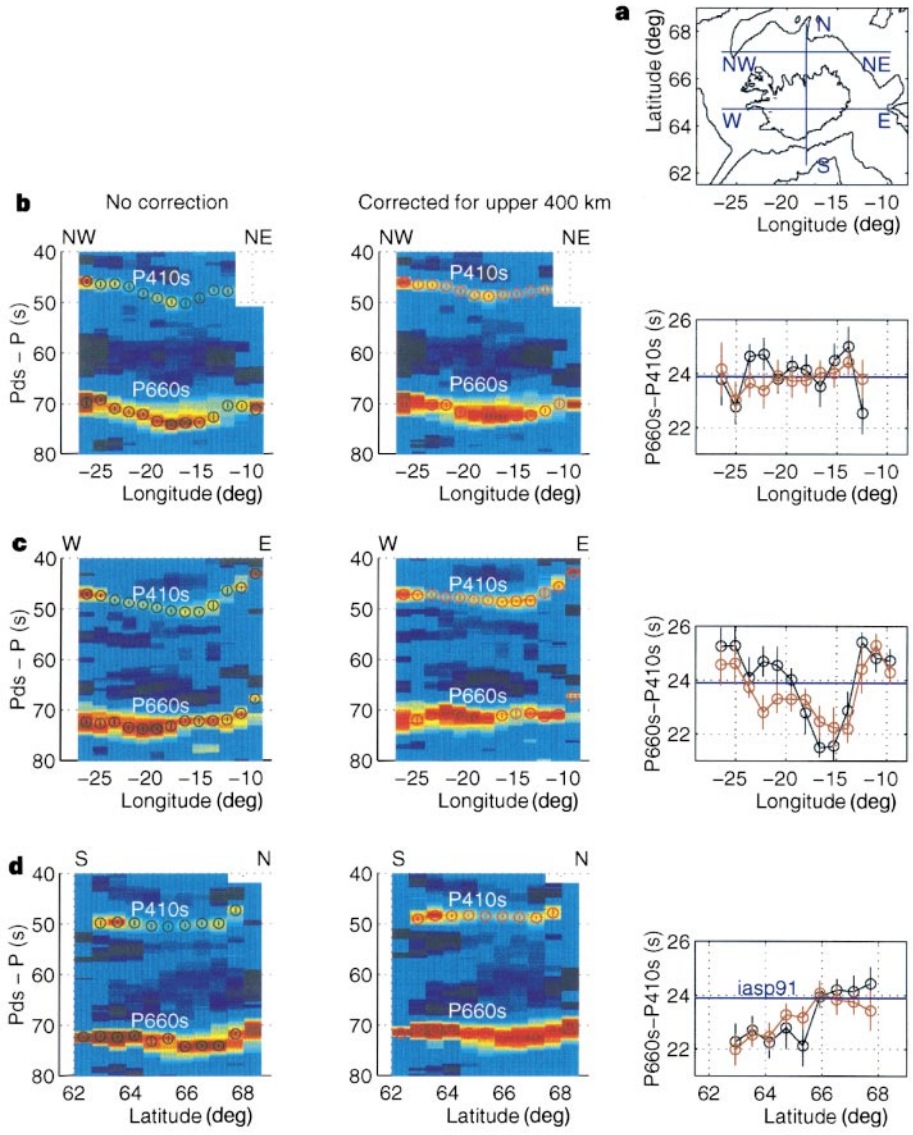

Figure 3 Images of P410s and P660s in stacked receiver functions and P660s-P410s differential times indicate an anomalously thin transition zone beneath central and southern Iceland. **a**, Locations of the profiles of receiver function stacks. **b**, The left-hand and middle panels display relative amplitudes of receiver function stacks along an east–west profile north of Iceland. Red and yellow colours represent positive and relatively higher-amplitude arrivals. We note that the *n*th-root stacking[16] amplifies weak signals in noisy data, but does not preserve amplitudes and waveforms. The vertical axis is the time after the compressional wave (P) arrival. Receiver functions are uncorrected (left panel) or have been corrected (middle panel) for the splitting of the converted phases and velocity heterogeneity in the upper 400 km. P660s-P410s differential times (right panel) are similar to that predicted for the iasp91 global model[9] (23.9 s, blue horizontal line) for both corrected (red circles) and uncorrected (black circles) receiver functions. The P410s and P660s times, the differential times, and their 1σ errors are estimated using a bootstrap method[30]. The relative amplitudes of identified P410s and P660s phases are greater than twice the levels of similarly processed and stacked records of noise immediately before the corresponding P arrivals. A 1-s change in differential time is equivalent to about a 10-km change in the transition zone thickness. **c**, An east–west profile through central Iceland. **d**, A north–south profile through central Iceland.

Nature © Macmillan Publishers Ltd 1998

Nature © Macmillan Publishers Ltd 1998

and d), where observed P660s-P410s differential times are less than that predicted by iasp91 by as much as 2.2 s. We applied corrections for velocity heterogeneity in the upper 400 km using P and S tomographic models[8] and for Pds shear-wave splitting using the results from SKS splitting analysis[18]. Station terms in the tomographic models[8] are incorporated, under the assumption that they reflect a uniform contribution from the upper 100 km. These corrections do not change the general pattern of differential times and only partially remove the effects of velocity heterogeneity (Fig. 3b), because the tomographic inversions underestimate the magnitude of the velocity anomalies[8]. Stacks of randomly selected receiver functions (see Supplementary Information) show significantly less coherence for the converted phases than the correctly binned stacks, indicating that the observed discontinuity structure is real.

The mantle transition-zone thickness beneath central and southern Iceland implied by the P660s-P410s differential times is less than beneath surrounding areas by ~20 km. The location and east–west dimension (400 km) of the region of the thinner (and therefore hotter than normal) transition zone (Fig. 4) are generally consistent with the location and diameter of the low-velocity anomalies at 300 km depth imaged in the tomographic models[8]. The mantle transition-zone thickness beneath the areas surrounding central and southern Iceland is comparable to that of the iasp91 model[9]. Observations of long-period SS precursors[17] indicate that the mantle transition zone in most oceanic areas is unlikely to be significantly thicker than in iasp91. This inference provides a basis for a discussion of the depth of origin of the Iceland plume.

The combination of a thinner transition zone beneath central and southern Iceland and a normal transition zone beneath surrounding areas is contrary to models in which the plume originates from an instability in a boundary layer at the base of the upper mantle as a result of regional heating from below[19,20] (Fig. 1c). Numerical and experimental studies have shown that the horizontal extent of the portion of the boundary layer supplying the thermal and mass flux at a plume is much greater than the diameter of the plume conduit[21]; in particular, the area of a conductive boundary layer 50–100 km thick supplying the plume would have to be 1,000–2,000 km in horizontal extent to match the excess heat flux at Iceland[22]. A broad

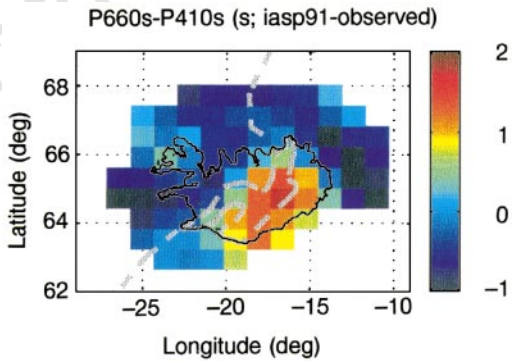

Figure 4 Map view of differences between the observed P660s-P410s differential times and the value predicted for the iasp91 model[9] underscores the localized nature of the anomaly. Receiver functions have not been corrected for shear-wave splitting or velocity heterogeneity in the upper 400 km; such corrections do not change the general pattern of differential times (Fig. 3 and Supplementary Information). Red and yellow colours indicate significantly smaller differential times (thinner mantle transition zone) than in iasp91, while blue colours denote normal or somewhat greater differential times (normal or slightly thicker mantle transition zone). The images have been smoothed by a two-dimensional, five-point moving average. The dashed grey lines delineate Icelandic neovolcanic zones and the axis of the Mid-Atlantic Ridge.

boundary-layer instability (Fig. 1c) having an excess temperature of 150–200 K (ref. 2) would reduce the depth of the 660-km discontinuity and the transition-zone thickness by 8–10 km (0.8–1.0 s differential P660s-P410s time) over a broad region, inconsistent with the normal transition-zone thickness observed beneath the areas surrounding central and southern Iceland.

The thinner transition zone appears to be circular within the mapped area and does not follow the geometry of the Mid-Atlantic Ridge (Fig. 4). This pattern suggests that a thinner transition zone is not a general feature of mid-ocean ridges. In support of this observation, receiver functions from sea-floor seismic stations on the southern East Pacific Rise[23] show that the average thickness of the underlying mantle transition zone is comparable to iasp91. Precursors to SS waves reflected beneath the northern East Pacific Rise show no significant difference between the transition-zone discontinuity depths beneath sea floor younger than 10 Myr and those beneath older sea floor[24]. Although the transition-zone thickness beneath the area southeast of Iceland remains to be mapped and we cannot fully rule out the possibility of a larger, regional anomaly, the fact that the thinner transition zone underlies the column of low seismic velocities in the tomographic models[8] and does not follow the ridge geometry suggests that the thinner transition zone is associated with the Iceland mantle plume.

Several lines of evidence, including tomographic images of subducting slabs penetrating the lower mantle in some areas[25] and the localized depression of the 660-km discontinuity beneath subduction zones[26,27], argue against a global thermal boundary layer above the 660-km discontinuity. Under two-layer mantle convection models, upwelling beneath spreading ridges would entrain anomalously hot material from such a boundary layer[28] and result in a deeper than normal 410-km discontinuity and a thinner than normal transition zone in the upwelling column, contrary to a normal mantle transition-zone thickness beneath most ridges. For strongly layered mantle convection models in which the depth of the 660-km discontinuity is nearly constant[5,19] (Fig. 1b), the low seismic velocities in the upper 400 km (ref. 8) and the thin and anomalously hot mantle transition zone beneath central and southern Iceland would result in greater delays to P660s arrivals in those areas; this is contrary to observations that P660s times beneath central and southern Iceland are less than beneath adjacent areas, except near the eastern and northern edges of the mapped region (Fig. 3c and d) where relatively greater average upper-mantle velocities appear to be present along the paths of the converted phases. Although the imaged discontinuity topography is affected either by no correction or by an undercorrection for velocity heterogeneity, corrections using seismic models with a narrower mantle plume and a larger velocity anomaly[8]—and including delays expected from higher than normal temperatures within the portion of the plume in the transition zone beneath central and southern Iceland (~0.2 s per 100 K excess temperature)—would only further shoal the apparent depth of the 660-km discontinuity and reduce the transition-zone thickness beneath central and southern Iceland.

Our observations are therefore most consistent with a lower-mantle origin for the Iceland plume (Fig. 1a). The variation in the depth to the 660-km discontinuity beneath Iceland is also consistent with our premise that the observed discontinuity corresponds to a mineralogical phase boundary, rather than a chemical boundary, because a chemically stratified boundary between the upper and lower mantle would be deflected by as much as several hundred kilometres by an upwelling plume[19,20] from the lower mantle. For Clapeyron slopes of 2.9 and −2.1 MPa K^{-1} for the 410- and 660-km discontinuities[29], respectively, the reduction of the transition-zone thickness by ~20 km beneath central and southern Iceland is equivalent to an excess temperature of 150 K, a result in good agreement with estimates of the thermal anomaly at the depth of melt generation (<200 km)[2]. The inferred excess temperature

Nature © Macmillan Publishers Ltd

Nature © Macmillan Publishers Ltd 1998

(150 K) and radius of the plume (200 km) should be regarded as lower and upper bounds, respectively, because the finite sizes of both the Fresnel zones of the converted phases and the patches used for stacking tend to smooth lateral variations in discontinuity depths (see Supplementary Information). These values nonetheless provide strong support for models of a hot and narrow plume penetrating the mantle transition zone beneath Iceland, and are similarly strong evidence against models in which the plume is broader (radius > 300 km) and has less excess temperature ($\Delta T \approx 70$ K)[3]. □

Received 9 September 1997; accepted 1 June 1998.

1. Schilling, J. G. Iceland mantle plume: Geochemical study of Reykjanes Ridge. *Nature* **242,** 565–571 (1973).
2. White, R. S., Brown, J. W. & Smallwood, J. R. The temperature of the Iceland plume and the origin of outward-propagating V-shaped ridges. *J. Geol. Soc. Lond.* **152,** 1039–1045 (1995).
3. Ribe, N. M., Christensen, U. R. & Theissing, J. The dynamics of plume-ridge interaction, 1: Ridge-centered plumes. *Earth Planet. Sci. Lett.* **134,** 155–168 (1995).
4. Morgan, W. J. Convection plumes in the lower mantle. *Nature* **230,** 42–43 (1971).
5. Richter, F. M. & McKenzie, D. P. On some consequences and possible causes of layered mantle convection. *J. Geophys. Res.* **86,** 6133–6142 (1981).
6. Anderson, D. L. Hotspots, basalts and the evolution of the mantle. *Science* **213,** 82–89 (1981).
7. Tryggvason, K., Husebye, E. S. & Stefánsson, R. Seismic image of the hypothesized Icelandic hot spot. *Tectonophysics* **100,** 94–118 (1983).
8. Wolfe, C. J., Bjarnason, I. Th., VanDecar, J. C. & Solomon, S. C. Seismic structure of the Iceland mantle plume. *Nature* **385,** 245–247 (1997).
9. Kennett, B. L. N. & Engdahl, E. R. Travel times for global earthquake location and phase identification. *Geophys. J. Int.* **105,** 429–466 (1991).
10. Nataf, H.-C. & VanDecar, J. Seismological detection of a mantle plume? *Nature* **364,** 115–120 (1993).
11. Liu, L.-G. in *Earth: Its Origin, Structure and Evolution* (ed McElhinny, M. W.) 177–202 (Academic, San Diego, 1979).
12. Langston, C. A. Structure under Mount Rainier, Washington, inferred from teleseismic body waves. *J. Geophys. Res.* **84,** 4749–4762 (1979).
13. Bjarnason, I. Th., Wolfe, C. J., Solomon, S. C. & Gudmundson, G. Initial results from the ICEMELT experiment: Body-wave delay times and shear-wave splitting across Iceland. *Geophys. Res. Lett.* **23,** 459–462 (1996); Correction. *Geophys. Res. Lett.* **23,** 903 (1996).
14. Shen, Y., Solomon, S. C., Bjarnason, I. Th. & Purdy, G. M. Hot mantle transition zone beneath Iceland and the adjacent Mid-Atlantic Ridge inferred from P-to-S conversions at the 410- and 660-km discontinuities. *Geophys. Res. Lett.* **23,** 3527–3530 (1996).
15. Dueker, K. G. & Sheehan, A. F. Mantle discontinuity structure from midpoint stacks of converted P to S waves across the Yellowstone hotspot track. *J. Geophys. Res.* **102,** 8313–8327 (1997).
16. Kanasewich, E. R., Hemmings, C. D. & Alpaslan, T. Nth-root stack nonlinear multichannel filter. *Geophysics* **38,** 327–338 (1973).
17. Shearer, P. M. Transition zone gradients and the 520-km discontinuity. *J. Geophys. Res.* **101,** 3053–3066 (1996).
18. Bjarnason, I. Th., Silver, P. G. & Solomon, S. C. Teleseismic shear wave splitting near the Iceland hotspot: Results from ICEMELT (abstr.). *Eos* **78,** S322 (1997).
19. Nakakuki, T., Sato, H. & Fujimoto, H. Interaction of the upwelling plume with the phase and chemical boundary at the 670 km discontinuity: Effects of temperature-dependent viscosity. *Earth Planet. Sci. Lett.* **121,** 369–384 (1994).
20. Kellogg, L. H. Interactions of plumes with a compositional boundary at 670 km. *Geophys. Res. Lett.* **18,** 865–868 (1991).
21. Olson, P., Schubert, G., Anderson, C. & Goldman, P. Plume formation and lithosphere erosion: A comparison of laboratory and numerical experiments. *J. Geophys. Res.* **93,** 15065–15084 (1988).
22. Sleep, N. H. Hotspots and mantle plumes: Some phenomenology. *J. Geophys. Res.* **95,** 6715–6736 (1990).
23. Shen, Y., Sheehan, A. F., Dueker, K. G., de Groot-Hedlin, C. & Gilbert, H. Mantle discontinuity structure beneath the southern East Pacific Rise from P-to-S converted phases. *Science* **280,** 1232–1235 (1998).
24. Lee, D.-K. & Grand, S. P. Depths of the upper mantle discontinuities beneath the East Pacific Rise. *Geophys. Res. Lett.* **23,** 3369–3372 (1996).
25. van der Hilst, R. D., Widiyantoro, S. & Engdahl, E. R. Evidence for deep mantle circulation from global tomography. *Nature* **386,** 578–584 (1997).
26. Wicks, C. W. & Richards, M. A. A detailed map of the 660-km discontinuity beneath the Izu-Bonin subduction zone. *Science* **261,** 1424–1427 (1993).
27. Niu, F. & Kawakatsu, H. Direct evidence for the undulation of the 660-km discontinuity beneath Tonga: Comparison of Japan and California array data. *Geophys. Res. Lett.* **22,** 531–534 (1995).
28. Zhong, S. & Gurnis, M. Role of plates and temperature-dependent viscosity in phase change dynamics. *J. Geophys. Res.* **99,** 15903–15917 (1994).
29. Bina, C. R. & Helffrich, G. Phase transition Clapeyron slopes and transition zone seismic discontinuity topography. *J. Geophys. Res.* **99,** 15853–15860 (1994).
30. Efron, B. & Gong, G. A leisure look at the bootstrap, the jackknife, and cross-validation. *Am. Stat.* **37,** 36–48 (1983).

Supplementary information is available on *Nature*'s World-Wide Web site (http://www.nature.com) or as paper copy from the London editorial office of Nature.

Acknowledgements. We thank Bjorn Bjarnason, Birgir Bjarnason, B. Brandsdóttir, H. Brynjlfósson, K. Egilsson, G. Gudmundson, E. Hannesson, T. Hardarson, L. Helgason, B. Ingimundarson, H. Jónsson, E. Kjartansson, A. Kuehnel, R. Kuehnel, P. Sigurdsson, R. Thrudmarsson, and the staff of the National Electric Company of Iceland (Landsvirkjun) for assistance with field operations; the IRIS-DMS for making available data from GSN station BORG; G. M. Purdy, D. W. Forsyth, R. S. Detrick, and J. A. Collins for encouragement and advice in the early stages of this work; S. van der Lee for providing software; D. E. James, E. M. Parmentier, I. S. Sacks, and P. G. Silver for discussions, and G. Helffrich and P. van Keken for reviews. This work was supported by the US NSF.

Correspondence and requests for materials should be addressed to Y.S. (e-mail: yshen@whoi.edu).

Microbiological evidence for Fe(III) reduction on early Earth

Madeline Vargas*, Kazem Kashefi, Elizabeth L. Blunt-Harris & Derek R. Lovley

Department of Microbiology, University of Massachusetts, Amherst, Massachusetts 01003, USA

It is generally considered[1] that sulphur reduction was one of the earliest forms of microbial respiration, because the known microorganisms that are most closely related to the last common ancestor of modern life are primarily anaerobic, sulphur-reducing hyperthermophiles[2–4]. However, geochemical evidence indicates that Fe(III) is more likely than sulphur to have been the first external electron acceptor of global significance in microbial metabolism[5–7]. Here we show that Archaea and Bacteria that are most closely related to the last common ancestor can reduce Fe(III) to Fe(II) and conserve energy to support growth from this respiration. Surprisingly, even *Thermotoga maritima*, previously considered to have only a fermentative metabolism, could grow as a respiratory organism when Fe(III) was provided as an electron acceptor. These results provide microbiological evidence that Fe(III) reduction could have been an important process on early Earth and suggest that microorganisms might contribute to Fe(III) reduction in modern hot biospheres. Furthermore, our discovery that hyperthermophiles that had previously been thought to require sulphur for cultivation can instead be grown without the production of toxic and corrosive sulphide, should aid biochemical investigations of these poorly understood organisms.

Our understanding of the geochemical conditions at the time when respiratory systems were first evolving suggests that the number of potential electron acceptors for microbial respiration was much more limited than at present. Important modern electron acceptors such as oxygen, nitrate and sulphate are unlikely to have been present in quantities sufficient to support globally significant rates of respiration[8,9]. However, Fe(III), derived from photochemical oxidation of Fe(II) in Archaean seas and from hydrothermal vent fluids, is thought to have been abundant on early Earth[5–7,10]. To examine whether Fe(III) reduction might have been a metabolic feature of ancient anaerobic microorganisms, various hyperthermophilic microorganisms were screened for their capacity for Fe(III) reduction. The rationale for this was that geochemical and microbiological evidence indicates that early life might have evolved in or near hydrothermal zones and thus extant hyperthermophilic microorganisms that are most closely related to the last common ancestor (LCA) may serve as models for early forms of microbial respiration[2,5,11,12]. Although a capacity for Fe(III) reduction has been found in a variety of microorganisms, including some moderate thermophiles[13–18], none of these is closely related to the LCA. Furthermore, the phylogenetic placement of these organisms in small, discrete groups does not provide convincing evidence for Fe(III) being an early metabolic characteristic[13].

All of the hyperthermophiles were found to reduce Fe(III) (Fig. 1). In each case, Fe(III) reduction was enzymatic as there was no Fe(III) reduction in controls without cells, or when cells were incubated at 35 °C, a temperature too low for hyperthermophilic enzymatic activity. The capacity for Fe(III) reduction was constitutive, as these organisms reduced Fe(III) even though they had been grown with other electron acceptors. This is similar to mesophilic Fe(III)-reducing bacteria, which also constitutively produce Fe(III) reductase when grown anaerobically with electron acceptors other than Fe(III)[14].

* Present address: Department of Biology, College of the Holy Cross, Worcester, Massachusetts 01610, USA

Nature © Macmillan Publishers Ltd 1998